

Assessing Behavior of Horizontal-Axis-Three-Blade Wind Turbines Under Tornadoes

*Mohamed AbuGazia^{1,2} Ashraf El Damatty^{1,3,4}, Kaoshan Dai³, and Wensheng Lu²

1) Department of Civil and Environmental Engineering, UWO, London, Ontario, Canada.

2) State Key Laboratory for Disaster Mitigation in Civil Engineering, Tongji University, Shanghai, China.

3) Department of Civil Engineering, Sichuan University, Chengdu, China.

4) Wind Engineering, Energy and Environmental Research Institute (WindEEE), UWO, London, Ontario, Canada.

ABSTRACT

High Intensity Wind (HIW) events have localized nature that makes analyzing Wind Turbines (WT) under tornadoes a challenging task. This notion stems from the fact that the tornado wind field is much more complicated compared to the synoptic boundary layer wind field as the tornado's 3-D velocity components vary significantly in space. Consequently, the supporting tower of the wind turbine and the blades will experience different velocities depending on the location of the event. Since wind turbines are typically designed to resist the synoptic wind loads as specified in current International Electrotechnical Commission (IEC) guidelines, it is found that these standards do not consider High-Intensity Wind (HIW) events such as tornadoes in the design stage. Therefore, a built-in-house numerical code "HIW-WT" has been developed to predict the straining actions on the blades and the tower considering the variability of the tornado's location and the blades' pitch angle. An extensive study has been conducted aiming to determine both the critical location of a tornado that will cause peak straining actions on the tower and blades, and the optimal pitch angle that will minimize the effects of that tornado. The minimum straining actions on the blades were found to occur when the pitch angles are 60°. A comparison of the simulation results with the extreme wind load scenario stated in the current IEC guidelines showed that the predicted straining actions on the blades, arising from the conditions specified in the IEC recommendations, are less than the straining actions due to F2 tornado.

1. INTRODUCTION

Steel tubular supporting towers are dominant in wind turbine production because steel is durable, ductile, and cost efficient until heights close to 80 m. Also, they have relatively smaller foundations compared to concrete towers. However, steel wind turbine towers are among the structures that are sensitive to HIW. This is because of the nature of the tubular tower and blades that makes the effect of localized HIW events, such as tornadoes, hazardous to either the tower body or the blades. Yet, the research investigations are not covering all the technical problems arising due to the increasing rate of constructing new wind farms. Consequently, structural failures of wind turbine towers have been reported lately around the world such as in the UK, Canada, Germany, and the USA. These failures indicate the need for more investigations regarding this issue. Accordingly, an extensive research program has been launched as a collaboration between Tongji University in China and the University of Western Ontario, Canada, to study various aspects related to this problem. The research included the development and validation of a three-bladed horizontal axis wind turbine tower's numerical model exposed to three-dimensional tornado wind fields based on numerical simulations. [Hamada et al., \(2010\)](#) developed a numerical model of a detailed transmission line system that accounted for the steel towers, insulators and the flexible conductors exposed to tornado wind fields while [Ibrahim et al., \(2018\)](#) developed a numerical model of a prestressed concrete pole exposed to both tornado and downburst wind fields. The main objective of the current study is to study the behavior of a wind turbine using a numerical model that is capable of predicting the critical tornado configuration that results in peak overturning moment acting on the wind tower and the peak root moment on each blade, while taking into account the variation in the tornado location (distance and orientation).

2. DESCRIPTION OF WIND TURBINE UNDER INVESTIGATION

The wind turbine considered in the current study is an S70/1500 three-blade horizontal axis wind turbine with a 1.5-MW capacity, a hub height of 65 m, and has a circular hollow steel tower that is 61.8 m high. The tower's base is 4 m in diameter with a thickness of 25 mm, while its top is 3 m in diameter and 10 mm thick. The tower is divided into 22 segments that correspond to the 22 welded steel segments, each with a different diameter and thickness. Each blade is 34 m long and is divided into 16 segments. The details of the wind turbine and its associated directions, which have been used in a series of studies previously, are shown in [Fig. 1](#).

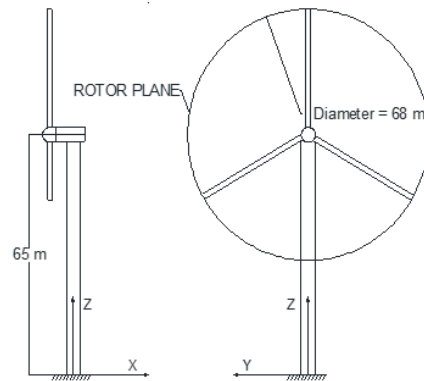


Fig. 1: Wind turbine tower under study

3. DESCRIPTION OF HIW-WT NUMERICAL CODE

This section discusses the development of the HIW-WT (High Intensity Winds on Wind Turbines) numerical code. For the current study, the wind field of an F2 tornado was obtained based on the CFD simulation conducted by [Hangan and Kim \(2008\)](#) for a swirl ratio of $S = 0.28$. The CFD simulation evaluated the spatial variation of the mean values of the tangential V_{TN} , radial V_{RD} , and vertical V_{ax} components of the wind field in a steady-state manner assuming smooth ground surface. The results of the simulation were validated through a comparison with the results of the small-scale experiments conducted by [\(Baker 1981\)](#). The simulation results were then calibrated based on full-scale data provided by [\(Sarkar et al. 2005\)](#) for an F4 tornado, and velocity and length scales were determined for that purpose accordingly. An F2 tornado was chosen for the current study because most of the tornadoes observed worldwide are F2 or less. In addition, designing a wind turbine tower for a tornado intensity stronger than F2 might not be an economical practice. [\(Hamada et al. 2010\)](#) concluded that the wind field produced by [\(Hangan and Kim 2008\)](#) with a swirl ratio $S=1$, can represent an F2 tornado after applying a length scale, $L_s = 4000$, and a velocity scale, $V_s = 13$. More details about the CFD simulation and the wind field properties can be found in [\(Hangan and Kim 2008\)](#), [\(Hamada et al 2010\)](#), [\(Hamada and El Damatty 2015\)](#) and [\(AbuGazia et al. 2020\)](#). The system of axes employed in the study for acquiring a sense of the spatial variations of the tornado wind field in a given space is illustrated in [Fig. 2](#), where the X- and Y-axes are located perpendicular and parallel to the rotor plane, respectively. Two variables, R and θ , define the location of the tornado for the current study, where R is the distance between the center of the tornado and the center of the base of the wind turbine tower, and θ is the orientation of the tornado (the angle between the Y-axis and the line that joins the center of the tornado and the tower).

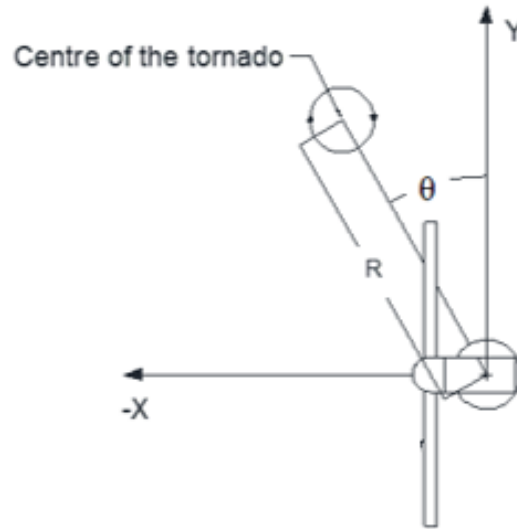


Fig. 2: Schematic of a tornado location for the current study relative to the centerline of the wind turbine

A force diagram is presented in **Fig. 3**, where Φ is the angle between the rotor plane and the chord line, α is the angle of attack of the wind, and β is the pitch angle of the blades.

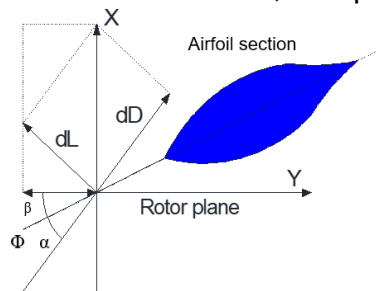


Fig. 3: Force diagram for a wind turbine blade element

The lift (dL) and drag (dD) forces on a random blade element (i) are calculated as follows:

$$dL_{ij} = (1/2) * (C_L)_{ij} * (\rho) * (c_i) * V_{ij}^2 \quad (1)$$

$$dD_{ij} = (1/2) * (C_d)_{ij} * (\rho) * (c_i) * V_{ij}^2 \quad (2)$$

where ρ is the air density, which is equal to 1.25 kg/m^3 , c_i is the chord length of the blade element (i), and V_{ij} is the wind velocity acting on the element, with (i) and (j) represent the element number and the direction of the wind velocity, respectively. $(C_L)_{ij}$ and $(C_d)_{ij}$ are the lift and drag coefficients, which vary depending on the geometry of element (i) and the wind direction (j).

For a pitch angle β , the attack angle α_j can be calculated from

$$\alpha_j = \Phi_j - \beta \quad (3)$$

Depending on the type of blade and its shape, the lift and drag coefficients are obtained as a function of the attack angle α_j . For a certain element (i), the tornado velocity components $(V_{TN})_i$, $(V_{RD})_i$, and $(V_{ax})_i$ are determined from the wind field based on its

radial coordinates (R and θ). Those are resolved using [Eq. 4 to 6](#) to obtain the velocity components (V_{ix} , V_{iy} , and V_{iz}) in the global directions.

$$V_{ix} = (V_{TN})_i (\cos \theta) + (V_{RD})_i (\sin \theta) \quad (4)$$

$$V_{iy} = (V_{TN})_i (\sin \theta) - (V_{RD})_i (\cos \theta) \quad (5)$$

$$V_{iz} = (V_{ax})_i \quad (6)$$

For element (i), [Eq. \(1\)](#), [\(2\)](#), and [\(3\)](#) are applied for the three velocity components V_{ix} , V_{iy} , and V_{iz} , respectively, to establish the drag and lift forces acting on each element. The wind loads acting on the body of the wind turbine tower are also calculated, based on the following equation:

$$F_{ij} = (1/2) * C_d * \rho * V_{ij}^2 * A \quad (7)$$

where C_d is the drag coefficient, taken equal to 1.2 for the tower (cylinder structure), and A is the projected area. In the final step, the blade forces can be resolved back into the plane of the blades and then used to determine the flapwise ($M_{flapwise}$) and edgewise moments ($M_{edgewise}$) at the roots of the blades. Once the forces on the blade elements have been calculated, the components of the overturning moments (M_{xx} and M_{yy}) as well as the torsional moment (M_{zz}) at the base of the tower can then be easily obtained. More details regarding the numerical model can be found in [\(AbuGazia et al. 2020\)](#). The analysis procedure is summarized in the flowchart presented in [Fig. 4](#).

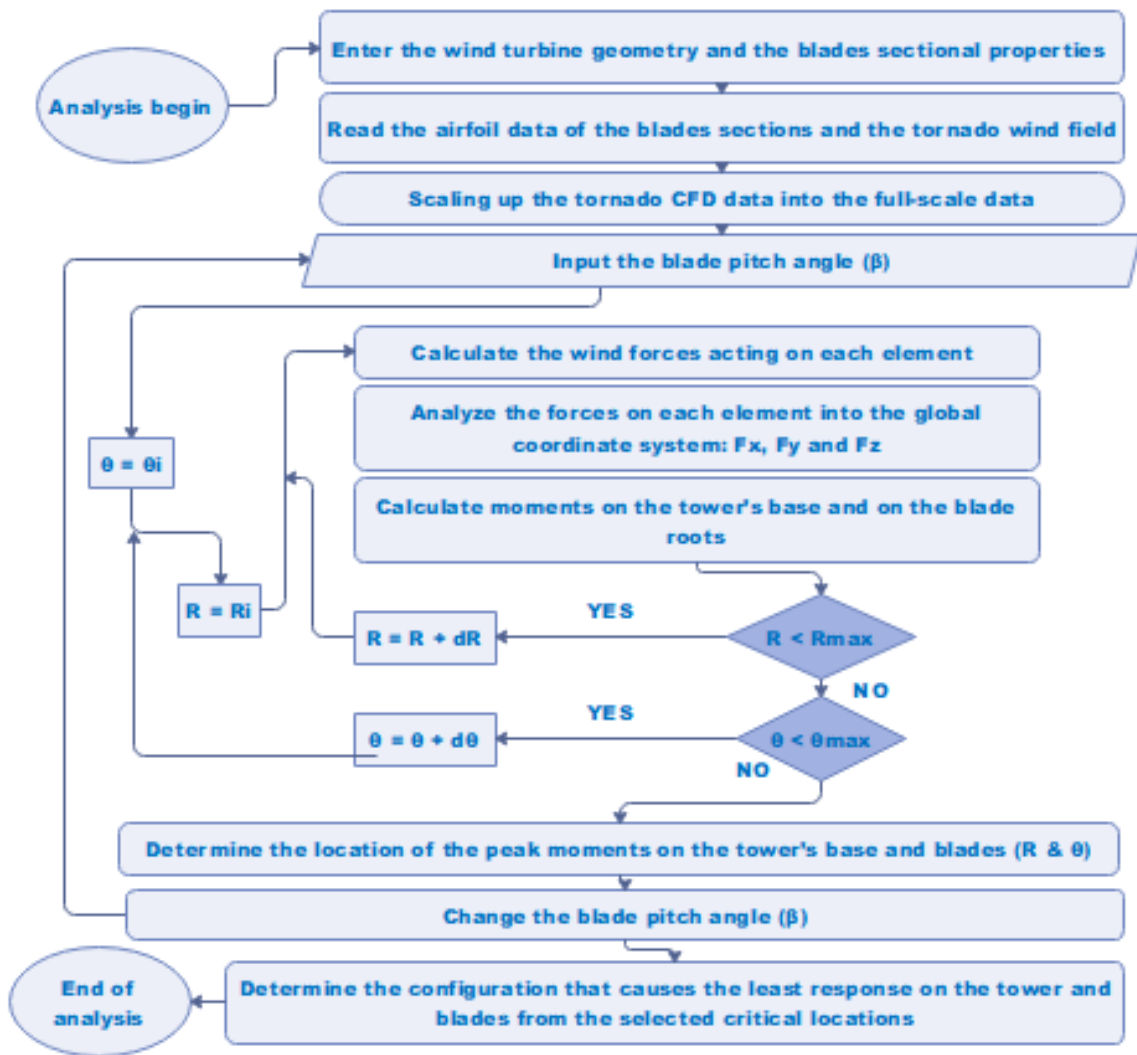


Fig. 4: Flowchart of the analysis procedure

To validate the developed HIWWT code, the values predicted by this code were compared with those produced by the **FAST simulation tool, (2018)**. Since the FAST software does not account for tornado loading, the validation of the code developed in this study was based on considering several separate one-dimensional wind fields as special cases of the 3-D wind field that can be done by HIWWT. The analysis was performed under different inflow wind speeds, yaw angles, and pitch angles. The inflow wind speeds were chosen to be 8 m/s, 10 m/s, 12 m/s, and 15 m/s, while the yaw angles were 0° and 90°, with 0° being in the X-direction and 90° being in the Y-direction. To reduce the effect of wind loads under high inflow wind speeds, it is recommended that the blades of the wind turbine be placed in a feather state, in which the pitch angle is 90°. Different pitch angles have been considered to take into account the interaction between pitch angles and velocity components of a tornado wind field. The comparison of the results shows a maximum difference in the range of 4-8 % for the root moments of the blades in the X-direction and 5-8 % in the Y-direction. For the moment of the tower base, the maximum difference between the two codes was found to be 7 % in the X-direction

and 11 % in the Y-direction. More details regarding the verification can be found in (AbuGazia et al. 2020).

4. CASE STUDY

Using the developed and validated code, a wind turbine was therefore analyzed. The tornado analysis involved a parametric study consisting of 1176 load cases that were examined using the developed code to represent an F2 tornado moving in space around the wind turbine tower, with varying radial distances R , circumferential angles θ , and pitch angles β for the blades. The radial distance R was set to range from 0 m to 288 m in 12 m increments, and the values of θ were selected to extend from 0° to 90° in 15° increments. IEC (2005) design recommendations were followed and applied for the wind turbine tower under study to compare the effects of the design loads and the F2 tornado loads. All load cases were included in consideration, and the appropriate safety factors were applied for the loads. For each pitch angle, 168 load cases were applied, producing a common trend. Figs. 5 shows the variation in the root moments of the three blades with changing radial distances R , for zero pitch angle β . The results are presented for different orientation angles θ . For all pitch angle configurations, the findings revealed that the straining action on the blades increases gradually with an increase in the radial distance R up to a specific limit, when the value then tends to decrease creating a bell curve shape. The maximum values for all β and θ were found to be within the range of $R = 144$ m to $R = 204$ m. For zero pitch angle, it is noted that the root moment of the vertical blade is the highest when the orientation of the tornado's wind field is zero, and decreases gradually with changing the orientation until it reaches the lowest value when the orientation is 90° as shown in Fig. 6. This happens because of the complexity of the tornado wind field as, at zero orientation, the higher component of the wind field (being the tangential component) acts exactly at the inflow direction (perpendicular to the rotor plane) where the projected area is the biggest, which results in a higher force on the elements and therefore a higher root moment. It is further noted that a contrary behavior occurs for 90° blade's pitch angle where the highest response is at 90° orientation and the least response occurs when the orientation between the tornado's wind fields (with Y-direction) is zero as shown in Fig. 7. This happens because the feathered blades during the parked condition are facing the tangential component of the wind field when the orientation angle is 90° which results in higher forces and therefore a higher root moment.

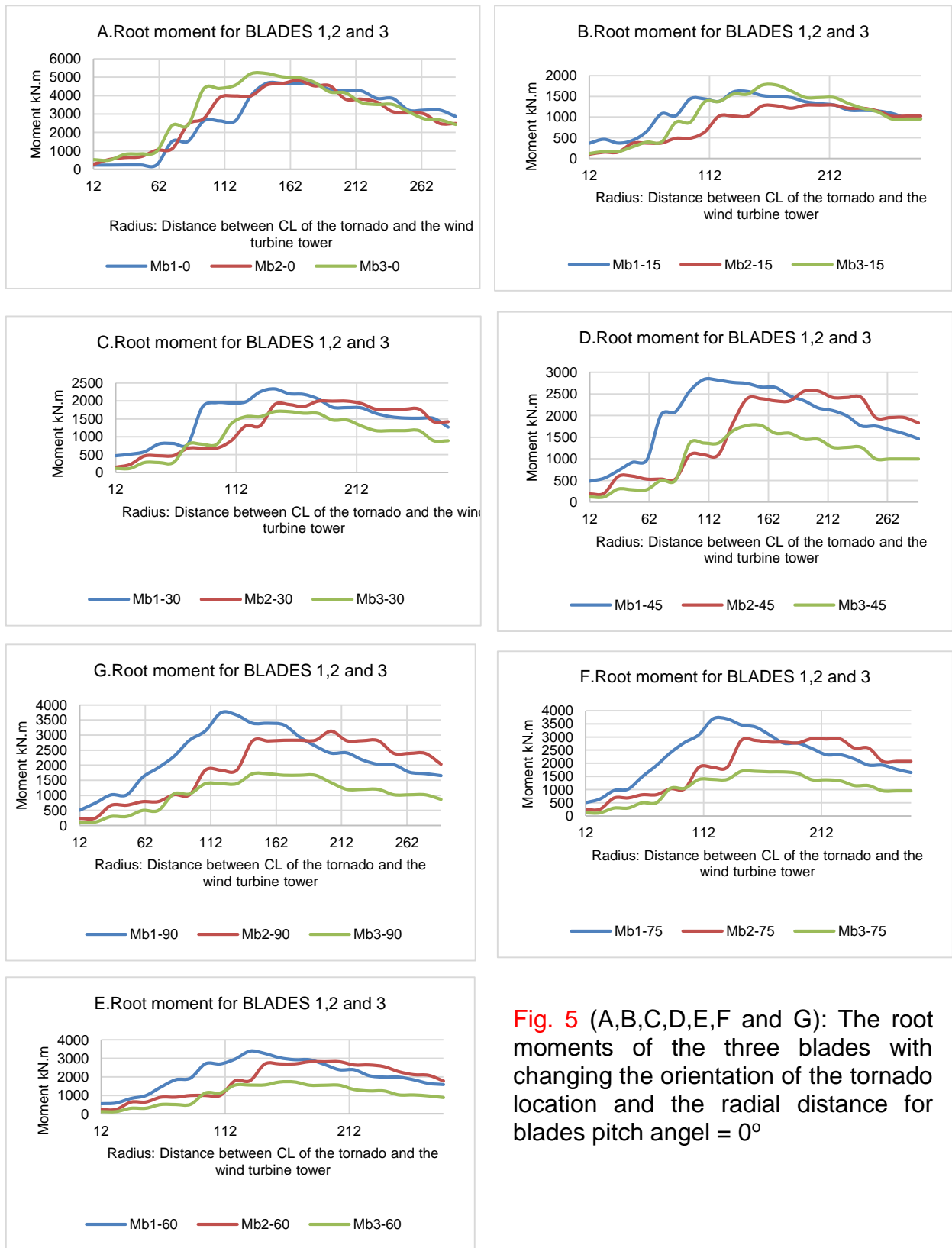


Fig. 5 (A,B,C,D,E,F and G): The root moments of the three blades with changing the orientation of the tornado location and the radial distance for blades pitch angle = 0°

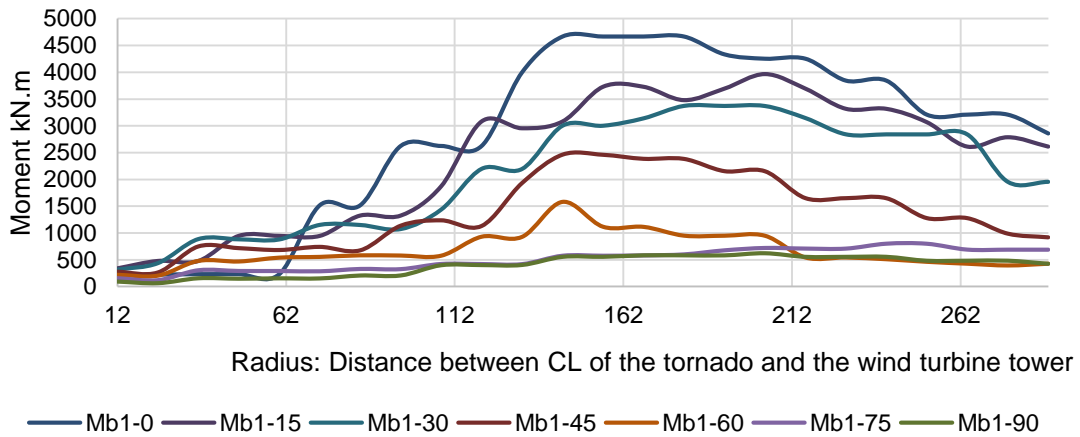


Fig. 6: Root moment for the VI. blade at pitch angle = 0°
 (with different orientation angles for the tornado)

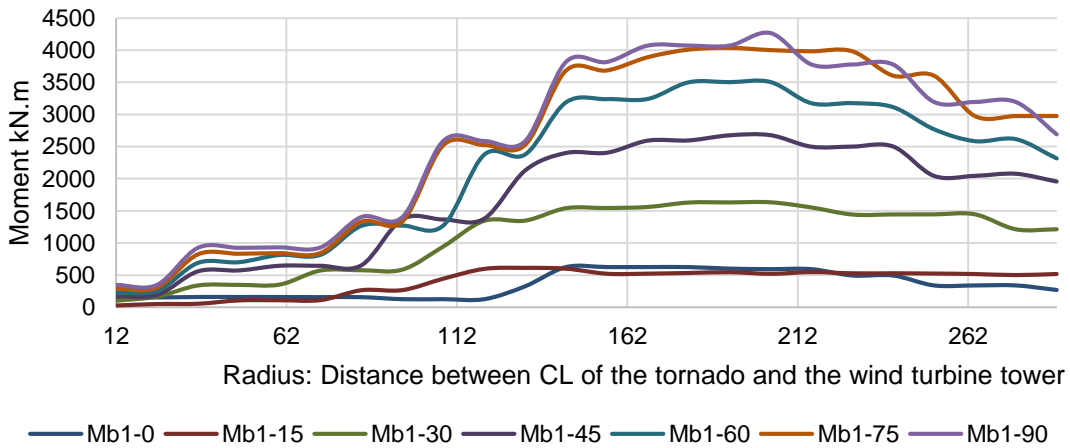


Fig. 7: Root moment for the VI. blade at pitch angle = 90°
 (with different orientation angles for the tornado)

As explained previously, the maximum values for all β and θ were found to be within the range of $R = 144$ m to $R = 204$ m. The results also indicated that $R = 168$ m produces a peak values for all β and θ . For this reason, $R = 168$ m was considered for the remainder of the study. To have a frame of reference, the moments are normalized using the values that correspond to the extreme synoptic wind results as explained in detail in (AbuGazia et al. 2020). To determine the pitch angle that results in the least straining actions on the blades, the maximum straining action for each pitch angle due to the movements of the tornado in the space around the wind turbine has been determined. The plots provided in Figs. 8 to 10 show the envelopes of the maximum straining actions for all pitch angles β . It was found that the overall maximum straining actions occur when the blade pitch angles are set to be 0° , with a gradual decrease in the straining action until the pitch angle is 60° . On the other hand, the minimum straining actions on the two inclined blades were found to occur when the pitch angles are set to be either 60° or 90° , which is in agreement with the recommendations to feather the blades when the wind turbine is exposed to high winds ($\beta = 90^\circ$). However, for the vertical blade, the minimum straining

action occurred only at $\beta = 60^\circ$, meaning that feathering the vertical blade during a tornado will increase the moment on the vertical blade, which makes it advisable to set it at $\beta = 60^\circ$.

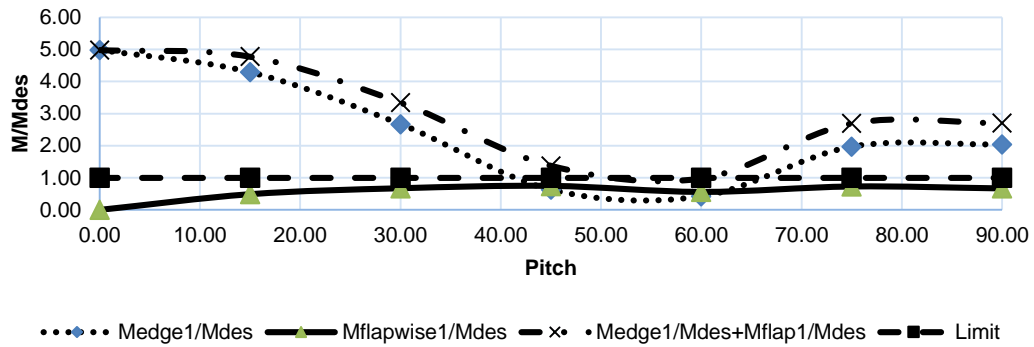


Fig. 8: Envelope of the maximum moments acting on Blade 1 at each pitch angle

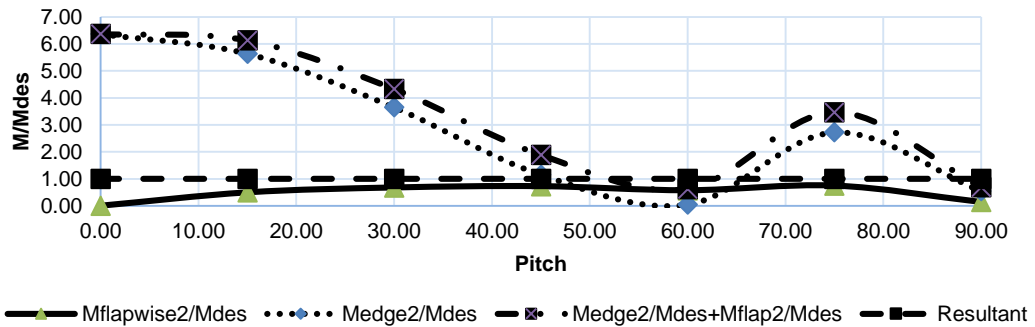


Fig. 9: Envelope of the maximum moments acting on Blade 2 at each pitch angle

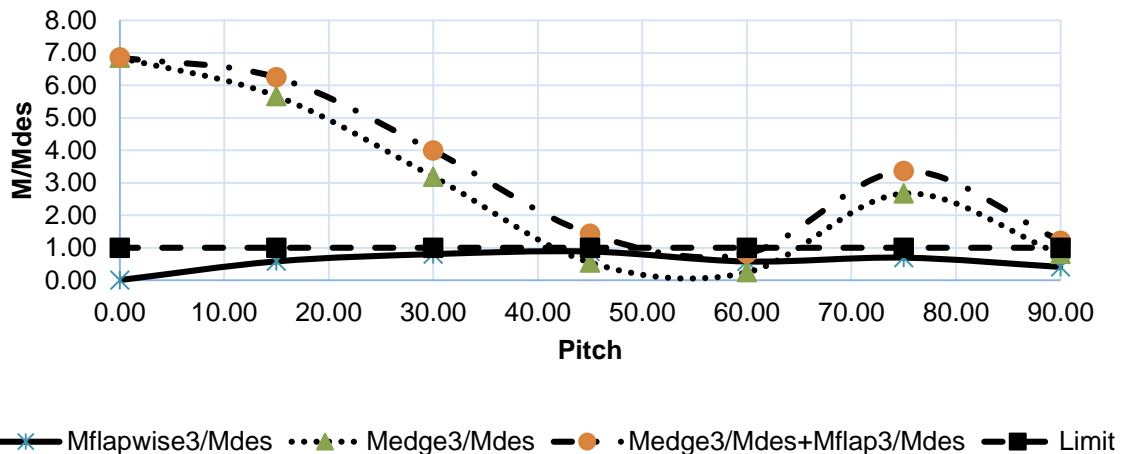


Fig. 10: Envelope of the maximum moments acting on Blade 3 at each pitch angle

Differences are also noted among the straining actions on the three blades for the same pitch angle, orientation, and radial distance. This observation can be attributed to the

axial component of the tornado, which has a significant effect on the inclined blades than on the vertical one. There are also differences between the two inclined blades themselves because of their different locations with respect to the center of the tornado: one blade is closer to the center and the other is farther away. Moreover, It was discovered that the highest overall straining action on the tower's base occurs when the blade pitch angles are set to be 75° at a radial distance of 168 m and an orientation angle of 75° , while the minimum takes place when the pitch angle is 15° and the orientation angle is 15° . The maximum base moments (resultant components) were normalized with the corresponding maximum straining values obtained from the design for $R = 168$ m. It is concluded that, for different pitch angles, the orientation angle resulting in the highest overall straining action on the tower base differs from the values determined in the case in which the maximum straining action on the blades was examined. This difference is attributable to the complexity of a tornado wind profile, which results in higher values for components near the ground and relatively smaller values for components at the hub height. A change in the direction of the radial component of the velocity relative to the height also has a significant effect on the base moments. For this reason, it is recommended to set the blade pitch angles at $\beta = 60^\circ$ and then to design the tower accordingly so that it can resist the additional straining action.

5. SUMMARY AND CONCLUSION

In this paper, a numerical model is applied to predict the response of wind turbines to tornado loading. The developed HIW-WT numerical model incorporates a wind field that was generated from a previously developed CFD model. The analyses are based on moving the tornado in space around the wind turbine to determine the critical tornado locations for both the tower and the blades for a variety of blade pitch angles. The following conclusions can be drawn:

- Changes in the tornado location and pitch angle lead to significant variations in the base moment of the tower and root moments of the blades.
- With the variability of the tornado location taken into account, the optimal pitch angle values corresponding to the minimum straining actions were found to be 60° for the vertical blade, 60° or 90° for the inclined blades, and 15° for the tower base.
- The values of the predicted straining actions on the blades calculated by the IEC are lower than the straining actions induced by the considered F2 tornado, except in the case of blades whose pitch angle $\beta = 60^\circ$.
- When the goal is to design the studied wind turbine so that it can sustain the wind field of the tornado presented herein, it is recommended that the blades be set to a pitch angle of $\beta = 60^\circ$, resulting in minimum moments on the blades. However, in this case, the tower must be designed to resist the straining actions associated with this pitch angle value.

Lastly, it has been found that the considered F2 tornado wind field presents a hazard for the investigated wind turbine and needs to be taken into account during the design stage to avoid unexpected load cases on the tower and the blades.

REFERENCES

- AbuGazia, M., El Damatty, A., Dai, K., Lu, W., Ibrahim, A., (2020). "Numerical Model for Analysis of Wind Turbines under Tornadoes", Engineering Structures, In press, Accepted July 2020.
- Baker, D. E. (1981), "Boundary layers in laminar vortex flows", Ph.D. thesis, Purdue University.
- Dai K., Sheng C., Zhao Z., Yi Z., Camara A, and Bitsuamlak, G., Nonlinear response history analysis and collapse mode study of a wind turbine tower subjected to cyclonic winds, *Wind & Structures*, 2017, **25**(1):79-100 .
- Fujita T.T., and A.D. Pearson, "Results of FPP classification of 1971 and 1972 tornadoes", 8th Conference on Severe Local Storms, USA, 1973.
- Fujita, T. Tornadoes and downbursts in the context of generalized planetary scales, *J. Atmos. Sci.*, 1981, **38**(8), 1511-1534.
- Hangan, H. and Kim, J., Swirl ratio effects on tornado vortices in relation to the Fujita scale, *Wind Struct.*, 2008, **11**(4), 291-302.
- Hamada A, El Damatty A A, Hangan H, Shehata A Y., Finite element modelling of transmission line structures under tornado wind loading. *Wind Struct*; 2010, **13**:451–69.
- Hamada A, El Damatty AA., Behaviour of guyed transmission line structures under tornado wind loading, *Comput Struct*; 2011, **89**:986–1003.
- Hamada, A. and El Damatty, A.A., Failure analysis of guyed transmission lines during F2 tornado event, *Engineering Structures*, 2015, **85**, 11-25.
- Ibrahim, A.M., El Damatty, A. A., and Elansary A.M., Finite element modelling of prestressed concrete poles under downbursts and tornadoes, *Journal of Engineering Structures*, 2017, **153**, 370-382.
- International Electrotechnical Commission, IEC, "Wind turbines – Part 1: Design requirements." 3rd ed. Standard IEC 61400-1, International Electrotechnical Commission, Geneva, Switzerland, 2005.
- Kaimal J.C., J.C. Wyngaard, Y. Izumi, and O.R. Cote, Spectral characteristics of surface-layer turbulence, *Q.J.R. Meteorol. Soc.*, 1972, v. **98**, pp. 563-598.
- NWTC Information Portal (FAST), National Renewable Energy Laboratory, Golden, CO, USA. <https://nwtc.nrel.gov/FAST>. Last modified 04-January-2018 ; Accessed 08-May-2020
- Sarkar, P., Haan, F., Gallus, W. Jr., Kuai, Le. and Wurman, J., Velocity measurements in a laboratory tornado simulator and their comparison with numerical and full-scale data, *Proceedings of the 37th Joint Meeting Panel on Wind and Seismic Effects (UJNR)*, Tsukuba, Japan, May, 2005.
- Zhi Zhao, Kaoshan Dai, Alfredo Camara, Girma Bitsuamlak, and Chao Sheng. Wind Turbine Tower Failure Modes Under Seismic and Wind Loads. *Journal of Performance of Constructed Facilities*, 2019, **33**(2): 04019015